Rotation studies in electron Internal Transport Barriers on TCV (BP8.00162)

L. Federspiel, B.P. Duval, O. Sauter, Y. Andrebe, S. Coda, A.N. Karpushov and the TCV team

École Polytechnique Fédérale de Lausanne (EPFL), Centre de Recherches en Physique des Plasmas, Association EURATOM-Confédération Suisse, CH-1015 Lausanne, Switzerland

I. Introduction - outline

- v_φ **and** v_{pol} **are measured with eITBs for the first time on TCV**
- **Effects of ECH power, co-/cnt-CD and MHD activity on the barrier strength, v,** E_r **and** $\omega'_{E\times B}$ **profiles are presented**
- $E\times B$ **shearing is not the cause of eITBs (confirms main role of reverse q profile for electron heating)**
- E_r **proportional to** ∇p_i **and** $\hat{\omega}$
- **Upgraded CXRS diagnostic on TCV with increased sensitivity and time resolution enables acquisitions near fast events**

II. CXRS diagnostic on TCV

- TCV is equipped with a **Charge eXchange Recombination Spectroscopy** (**CXRS**) diagnostic
- CX reaction: C^{6+} (plasma) + neutral H^0 (low power **Diagnostic Neutral Beam Injector**, **DNBI**) ⇒ **CVI line (n=8→7,** λ **=529.1 nm)**
- **Carbon** main impurity in TCV (C wall) → thermalised with main ion species (D or H)
- Collected light spectroscopically analysed → T_i, n_C, v_φ and v_{pol} (v_θ) profiles of C ions along the vessel mid-plane
- **DNBI** injects 50 keV-H^0 atoms in 10-30 ms bursts at z=0 cm (Act./Pas.: 5-100%)
- 3 **CXRS** observation systems covering the plasma core and edge:
  - Toroidal Low Field Side (TLFS)
  - Toroidal High Field Side (THFS)
  - Poloidal Low Field Side (PLFS)
- 3 × 40 observation chords arranged in pairs (Double Slit configuration)
- Toroidal systems radial resolution of ∼ 1.5 cm
- ***Standard Acquisition***: t_{int}= 10-30 ms → $t_{resolution}$= 20-90 ms
- **Plasmas** vertically centered around z=0cm

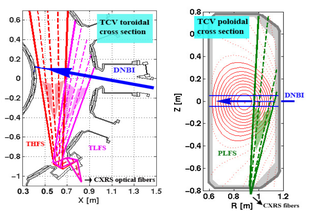

III. CXRS present state (2011-2012 upgrade)

- Installed 2 **Andor** ^{TM} **iXon** $^{EM+}$ **DU897D-CSO-BV** cameras
  - Back illuminated e2v CCD97 detectors with **Electron Multiplying (EM) gain** up to 300
  - PreAmplifier Gain: ×1 − ×5
  - CCD image area 8.2 × 8.2mm^2 with 16 μm pixel size
  - Quantum efficiency: 95 %
  - Frame transfer time: 0.25 ms
  - Integration time in 512 × 20 frame transfer format: 1.7 ms

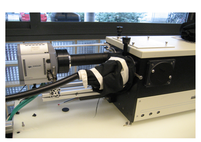

- **Improved time resolution: 40 chords full range acquisition less than 2 ms!**
- **Increased sensitivity:** ×8 **better S/N ratio!**
  - ***TCV***: low power DNBI perturbs only slightly the plasma (externally applied torque neglected)
    - v_C ≈ **intrinsic ion rotation (ITER like)**
    - Beam traverses the whole plasma BUT **limited** active signal intensity!
  - ***Other devices***: high power NBI perturbs v_C profiles dominated by applied torque
- **Standard triggering**:
  - CXRS acquisition synchronized with DNBI pulses (ramp up triggering)
  - Real Time (RT) - control sawteeth (ST) trigger modulation to stabilise ST frequency

⇒ **Enlarged CXRS exploitation**: detect faster events (∼ few ms) in scenarios where beam strongly attenuated and active signal weaker or much more irregular (eITBs or n_e ramp in H-modes)

IV. Electron Internal Transport Barriers (eITB) on TCV

- **eITBs** formed using Electron Cyclotron Heating and Current Drive (ECH/ECCD, X2 @ 82.7 GHz) to create hollow or flat current profiles [1]
- ***TCV***: key ingredient for eITB formation and sustainment is the **degree of reverse shear** [2]
- ***Other devices***: rational q and/or the $E\times B$ shearing
- Study effect of ECH power, MHD activity on the barrier strength, v, E_r and $\omega'_{E\times B}$ profiles
  ↪ CXRS: v profiles during stationary pre-barrier, sustainment and rapid formation phases in single discharge

V. eITB targets development at z=3 cm on TCV

CENTRAL INTERNAL BARRIER TARGET (ICEC) [3]:

- **Central cnt-CD** with **off-axis co-ECCD**
- Δz = 15 cm, $n_e = 1.8\times10^{19}m^{-3}$
  T_e = 6 keV, H_{RLW} = 2.9
- **Barrier in** T_e **but not** n_e

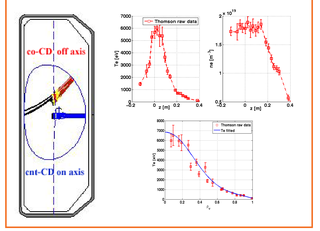

CO-ECCD eITB TARGET:

- **Off-axis co-ECCD** with **central ECH** & **central co-CD** (stronger and more off axis barrier than central eITB, 2300kW)
- Δz = 15 cm, $n_e = 1.8\times10^{19}m^{-3}$
  T_e = 4.5 keV, $H_{RLW} = 2.5 \rightarrow 2.8$
- RT IOH control dI_{OH}/dt
- Reduce high n_e & impurity in TCV

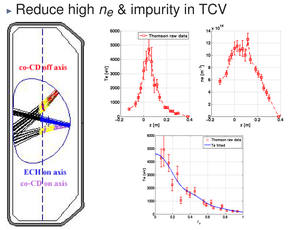

VI. Rotation, E_r & $E\times B$ shearing rate profiles vs MHD activity

- **Barrier destroyed by MHD activity**: MHD mode (2,1) @ 7kHz + stronger mode
- Barrier ⇒ **cnt-current (Ip) toroidal rotation** (v_φ)
- **MHD mode ⇒ rotation reversal co-Ip** v_φ
- Strong mode ⇒ **relaxation to cnt-Ip** v_φ (≅ OH) and decrease in the core
- $E_r < 0$ is **inward** during barrier
- MHD mode causes E_r sign change in the core (outward)

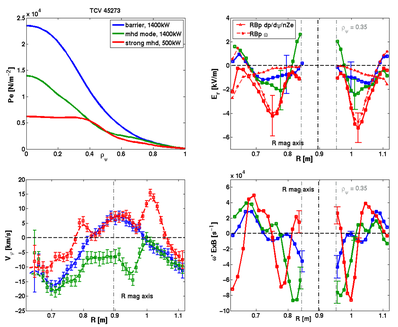

⇒ **MHD activity strong effect on** v_φ **and** E_r **profiles**
⇒ **minimum** E_r **(strong** $\hat{\omega}R\tilde{B}_{pol}$ **component)** ↔ $\omega'_{E\times B} = 0$ **at midradius**

VII.Effect of central ECH power on the central barrier strength

OH, central cnt-ECCD (central eITB) & co-CD (730kW)

- Cnt-CD ↔ co-CD (similar to central ECH): peaked cnt-Ip v_φ in the core with **doubled** v_φ **and** p_e
- p_e increases inside $\rho_\psi = 0.5$ ⇒ confinement improvement (barrier) [4]
- p_e ⇒ clear difference in the electron transport!
- v_φ increases for $\rho_\psi < 0.45$
- $E_r < 0$ **inward** (-2 kV/m): **smaller for cnt-CD** than co-CD
- $E\times B$ **shearing rate** for cnt-CD and co-CD is **similar** in both cases

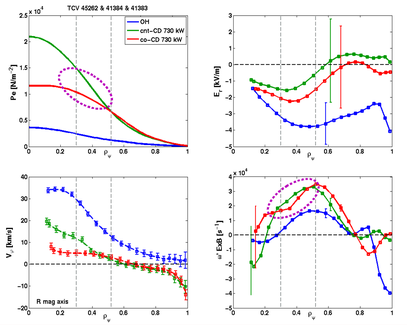

⇒ $E\times B$ **shearing rate not the cause of electron transport improvement**
⇒ **BUT increased** v_φ **profile for central eITB may result from improved confinement**

VIII. Rotation, E_r & $E\times B$ shearing rate profiles vs total power

ECH total power scan & OH

- Central cnt-Ip v_φ
- **Inboard-outboard** v_φ **asymmetry**
- v_φ **increases** & E_r **decreases** when reducing the ECH power
- $E_r < 0$ **inward** (-[1,4]kV/m) and deeper in the core ($\hat{\omega}R\tilde{B}_{pol}$ term)
- $c_{si} = \sqrt{\frac{T_0(500eV)}{m_D}} \cong 1.5\times10^5 m/s$
- $c_{si}/R_0 \cong 1.8\times10^5 s^{-1}$
- **TEM modes most instable** in TCV eITB plasmas
- $\gamma R_0/c_{si} = 0.4$ [5]

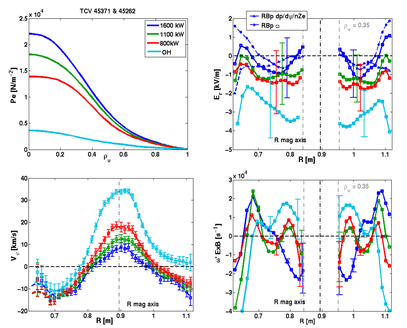

⇒ $\omega'_{E\times B} \propto 10^4 s^{-1}$ **smaller compare to** $\gamma \propto 10^5 s^{-1}$ **of TEM**
⇒ **Consistent with assumed negligible effect of** $\omega'_{E\times B}$ **on TEM in TCV reverse shear [6,7]**

XI. Conclusions

- **Effects of ECH power, co-/cnt-CD and MHD activity on the barrier strength, v,** E_r **and** $\omega'_{E\times B}$ **profiles are presented**
- v_φ **AND** v_{pol} **are measured with eITBs for the first time**
- $E\times B$ **shearing is not the cause of eITBs (confirms main role of reverse q profile for electron heating)**
- $E_r \sim \nabla p_i$ **and** $\hat{\omega}$
- **Upgraded CXRS diagnostic on TCV enables acquisition near fast events**

IX. u_{pol} indirect measurement, E_r & $E\times B$ shearing rate

Tokamak Coordinate Conventions [8, 9]:

- **COCOS=17**
- $I_p, B_0, B_{pol} > 0$
- $\hat{\omega} > 0$, $\hat{u} > 0$
- $u_\varphi > 0$, $u_{pol} < 0$

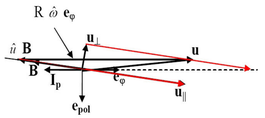

Poloidal and toroidal rotation indirect measurement ($\hat{u}(\Psi)$, $\hat{\omega}(\Psi)$,$K(\Psi)$ **flux functions):**

$$\mathbf{u}_\sigma = \hat{u}_\sigma(\Psi)\mathbf{B} + R\hat{\omega}_\sigma(\Psi)\mathbf{e}_\varphi$$
$$u_{\sigma\varphi} = R\hat{\omega}_\sigma(\Psi) + \hat{u}_\sigma(\Psi)B_\varphi$$
$$u_{\sigma pol} = \hat{u}_\sigma(\Psi)B_{pol} = \sigma_{\rho\theta\varphi}\sigma_{Ip}\hat{u}_\sigma(\Psi)\tilde{B}_{pol}$$

where $\tilde{B}_{pol} = \left|B_{pol}\right|$, $B_\varphi = F/R$. Using R_H & R_L on the same flux surface:

$$\hat{\omega}(\Psi) = \frac{u_{\varphi,H}R_H - u_{\varphi,L}R_L}{R_L^2 - R_H^2} \qquad \hat{u}(\Psi) = \frac{u_{\varphi,H}/R_H - u_{\varphi,L}/R_L R_L^2 R_H^2}{R_L^2 - R_H^2}\frac{R_H^2}{F}$$

when impurity asymmetry can not be neglected:

$$n(\Psi,\theta)\hat{u}(\Psi,\theta) = K(\Psi) = \frac{1}{F}\left(\frac{u_{\varphi,H}}{R_H} - \frac{u_{\varphi,L}}{R_L} - \sigma_{Bp}(2\pi)^{e_{Bp}}\frac{T}{Ze}\frac{\partial ln(n_H/n_L)}{\partial\Psi}\right)\times\left(\frac{n_L n_H R_L^2 R_H^2}{n_L R_L^2 - n_H R_H^2}\right)$$

Radial electric field:

$$\mathbf{E} = \frac{1}{n_\sigma Ze}\nabla p_\sigma - \mathbf{u}_\sigma\times\mathbf{B} \qquad \frac{\mathbf{E}\cdot\nabla\Psi}{|\nabla\Psi|} = \left[\frac{1}{n_\sigma Ze}\frac{dp_\sigma(\Psi)}{d\Psi} + \hat{\omega}_\sigma(\Psi)\frac{\sigma_{Bp}}{(2\pi)^{e_{Bp}}}\right](2\pi)^{e_{Bp}}R\tilde{B}_{pol}$$

$$E_r = \left[\frac{(2\pi)^{e_{Bp}}}{n_\sigma Ze}\frac{dp_\sigma}{d|\Psi-\Psi_{axis}|} + \hat{\omega}_\sigma(\Psi)\sigma_{Ip}\right]R\tilde{B}_{pol} \qquad E_r(\rho_\psi = 0) = 0$$

where $d\Psi = \sigma_{Bp}\sigma_{Ip}d\left|\Psi - \Psi_{axis}\right|$

$E\times B$ **shearing rate [10]:**

$$\omega'_{E\times B} = \frac{r}{q_s B_0}\frac{d}{dr}\left(\frac{q_s E_r}{r}\right)$$

X. Agreement between measured V_φ,V_{pol} and indirect u_φ,u_{pol}

Calculated $\hat{\omega}$ **&** $\hat{u}$ **(TCV 45371)**

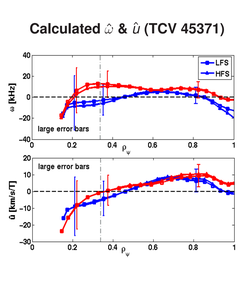

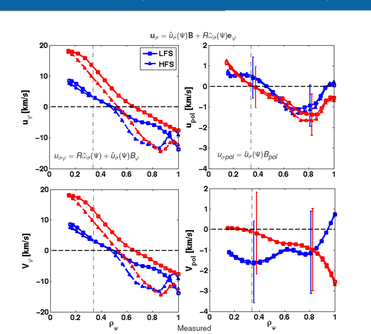

References:

- [1] S. Coda et al., *Nucl. Fusion*, **47**, 714-720 (2007)
- [2] O. Sauter et al., *Phys. Rev. Letters*, **94**, 105002 (2005)
- [3] Z.A. Pietrzyk et al., *Phys. Rev. Letters*, **86**, 1530 (2001)
- [4] O. Sauter et al., *23rd IAEA Conference*, paper EXS/P2-17 (2010)
- [5] X. Lapillonne et al., *EPFL thesis*, **4684**, (2010)
- [6] T. Gorler et al., *PoP*, **18**, 056103 (2011)
- [7] A. Bottino et al., *PPCF*, **48**, 215-233 (2006)
- [8] O. Sauter et al., *Comput. Phys. Commun.*, **doi: 10.1016/j.cpc.2012.09.010**, (2012)
- [9] A. Bortolon et al., *Accepted to Nucl. Fusion*,(2012)
- [10] T. Vernay et al., *PoP*,**19**, 042301 (2012)

This work was partly supported by the Swiss National Science Foundation.

lucia.federspiel@epfl.ch